

High velocity features in the spectra of the Type Ia SN 1999ee: a property of the explosion or evidence of circumstellar interaction?

P. A. Mazzali^{1,2,3,4*}, S. Benetti⁵, M. Stehle^{4,6}, D. Branch⁷, J. Deng^{2,3},
K. Maeda^{2,3}, K. Nomoto^{2,3}, M. Hamuy⁸

¹*INAF-Osservatorio Astronomico, Via Tiepolo, 11, I-34131 Trieste, Italy*

²*Department of Astronomy, University of Tokyo, Bunkyo-ku, Tokyo 113-0033, Japan*

³*Research Center for the Early Universe, University of Tokyo, Bunkyo-ku, Tokyo 113-0033, Japan*

⁴*Max-Planck Institut für Astrophysik, Karl-Schwarzschildstr. 1, D-85748 Garching, Germany*

⁵*INAF-Osservatorio Astronomico, vicolo dell'Osservatorio, 5, I-35122 Padova, Italy*

⁶*Universitäts-Sternwarte München, Scheinerstr. 1, D-81679 München, Germany*

⁷*Astronomy Dept., Univ. of Oklahoma, Norman, OK, USA*

⁸*Observatories of the Carnegie Institution of Washington, 813 Santa Barbara Street, Pasadena, CA 91101-1292, USA*

Accepted ... Received ...; in original form ...

ABSTRACT

The near-maximum spectra of the Type Ia SN 1999ee are reviewed. Two narrow absorption features corresponding to the strongest component of the Ca II IR triplet appear in the spectra from 7 days before to 2 days after B -band maximum, at a high velocity ($\sim 22,000 \text{ km s}^{-1}$). Before these features emerge, the Ca II IR triplet has an anomalously high velocity, indicating that the narrow features were still blended with the main, photospheric component. High-velocity Ca II absorption has been observed in other SNe Ia, but usually detached from the photospheric component. Furthermore, the Si II 6355Å line is observed at a comparably high velocity ($\sim 20,000 \text{ km s}^{-1}$) 9 and 7 days before B maximum, but then it suddenly shifts to much lower velocities. Synthetic spectra are used to reproduce the data under various scenarios. An abundance enhancement requires an outer region dominated by Si and Ca, the origin of which is not easy to explain in terms of nuclear burning. A density enhancement leads to a good reproduction of the spectral evolution if a mass of $\sim 0.10M_{\odot}$ is added at velocities between 16,000 and 28,000 km s^{-1} , and it may result from a perturbation, possibly angular, of the explosion. An improved match to the Ca II IR triplet at the earliest epoch can be obtained if the outermost part of this modified density profile is assumed to be dominated by H ($\sim 0.004M_{\odot}$ above 24,000 km s^{-1}). Line broadening is then the result of increased electron scattering. This H may be the result of interaction between the ejecta and circumstellar material.

Key words: supernovae: general — supernovae: individual (SN 1999ee)

1 INTRODUCTION

Having become extremely fashionable for their role as standardisable cosmological candles, Type Ia Supernovae (SNe Ia) are becoming the centre of a kind of scientific industry, with large programmes, both observational and theoretical, being launched to explore their properties, detect them at all redshifts, and understand the physical properties of the explosion and the mechanism that holds the key to their apparent predictability. Since the main observational feature

– the brightness–decline rate relation, is a one-parameter relation (Phillips 1993), and because most modelling work has been performed in 1D, it was typically assumed that the ejecta of SNe Ia are homogeneous, with little or no deviation from smooth density profiles and spherical symmetry. Recently, however, some suggestion that these assumptions may not always be correct has come from polarisation measurements (Wang et al. 2003). Another, possibly related finding, is the detection of detached, high-velocity components in near-maximum spectra.

The first suggestion of high-velocity components was made by Hatano et al. (1999), who noticed features that

* E-mail: (PAM) mazzali@ts.astro.it

they interpreted as high-velocity Ca II and Fe II in the spectra of SN 1994D. They showed through spectral modelling that Ca II and Fe II are present at $v > 25000 \text{ km s}^{-1}$, and reaching $v = 40000 \text{ km s}^{-1}$, detached from the photospheric component ($v < 16000 \text{ km s}^{-1}$). Further evidence came from SN 2000cx (Li et al. 2001), which shows two strong and well separated components of the Ca II IR triplet at high velocities. Thomas et al. (2004) analysed the spectra of this rather peculiar SN Ia, using a simple 3D spectrum synthesis model. They confirmed that detached Ca II is present at high velocities, this time $v > 16000 \text{ km s}^{-1}$. They also noticed a corresponding broadening of the Ca II H&K doublet, which however did not show detached features. Recently, Branch et al. (2004) confirmed these findings, and additionally reported that high-velocity Ti II features are also present. Detached features were also observed in SN 2001el (Wang et al. 2003) at $v \sim 22 - 26000 \text{ km s}^{-1}$, in SN 2003du at $v \sim 18000 \text{ km s}^{-1}$ (Gerardy et al. 2004), and in SN 2004dt (F. Patat, priv. comm.).

In this paper we present and discuss evidence for a high-velocity component that is present in the spectra of another otherwise normal SN Ia, SN 1999ee (Hamuy et al. 2002; Stritzinger et al. 2002). We argue in this case that not only Ca II and possibly Fe II show high-velocity features, but that a sudden change in the shape of the profile and the position of Si II 6355Å, the characterising line of SNe Ia, is due to the presence (and progressive thinning out) of a high-velocity Si component, which is identified for the first time in a SN Ia. Since the presence of Si has major implications for the properties of the explosion, we model the time-evolution of the spectra in order to identify the nature of the discontinuity giving rise to the high-velocity feature (abundance, ionisation, density, interaction with circumstellar material), and to quantify the amount of high-velocity material, in particular Si, required to reproduce the observations.

2 EVIDENCE FOR HIGH-VELOCITY FEATURES IN THE SPECTRA OF SN 1999EE

Optical and infrared spectra of SN 1999ee covering the period from -9d to +42 days relative to B maximum were presented by Hamuy et al. (2002). SN 1999ee is a rather slow-decliner ($\Delta m_{15}(B) = 0.91$), but it does not show the spectroscopic peculiarities of SN 1991T and similar SNe. The spectral evolution and line identification are discussed by Hamuy et al. (2002).

Although the spectra of SN 1999ee look like those of a typical SN Ia, the Ca II IR triplet shows two small notches, separated by exactly the line separation of the two strongest components ($\lambda 8542$ and 8662\AA). The narrow features are first visible on day -2, and persist until day +3, during which time their position does not change significantly, indicating that they are formed in a layer that is detached above the photosphere, with central velocity $\sim 22000 \text{ km s}^{-1}$. This is similar to the SNe Ia discussed above, although in SN 1999ee the narrow features are not clearly separated from the main broad absorption, which is of photospheric origin. If these features are correctly identified, their weakness in the two earlier spectra (day -9 and -7) could result from the fact that

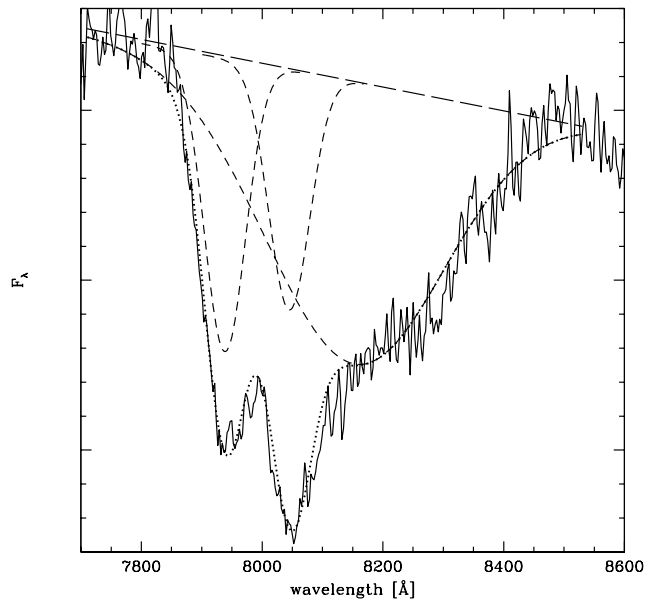


Figure 1. Decomposition of the absorption part of the Ca II IR triplet into three gaussian components. The broad component is the blended photospheric feature, while the narrow ones are the high-velocity absorptions of the two strongest lines in the triplet.

the photosphere at those early epochs was located at velocities comparable to that of the narrow features. These would therefore blend almost completely with the broad component, resulting in a very broad Ca II IR triplet, as is indeed observed. The later disappearance of the narrow features, going from day +3 to day +8, is then the combined consequence of the decreasing density in the high-velocity zone caused by expansion and of the inward motion of the photosphere, which becomes removed from the detached Ca II zone. Fig. 1 shows how the Ca II IR triplet can be decomposed into three different components, one broad and two narrow. Fig. 2 shows the time evolution of the central velocity of each component. The broad photospheric absorption drops rather smoothly from 20000 to 15000 km s^{-1} , but the two detached features are clearly measured at velocities between 24000 and 20000 km s^{-1} and then disappear.

There is however another piece of observational evidence, not as clear perhaps as that of the Ca II IR triplet but certainly at least as rich in physical implications: the sudden change in the shape of the Si II 6355Å line between day -7 and day -2. In the two earliest spectra, the line appears unusually blue (with a central wavelength of $\sim 6000 \text{\AA}$, indicating a velocity of $\sim 16000 \text{ km s}^{-1}$). Additionally, it displays a P-Cygni profile which increases in strength towards the highest velocities, both in absorption and in emission, which is unusual for SNe Ia lines. After this phase, the line moves suddenly to the red, and it looks like a perfectly normal SN line on day +3. The velocity evolution of the Si II line is also shown in Fig. 2. After the sudden drop, the velocity of the line continues to decrease, but at a much lower rate.

The coincidence in time of the appearing of the Ca II narrow features and the redward shift of the Si II line, and

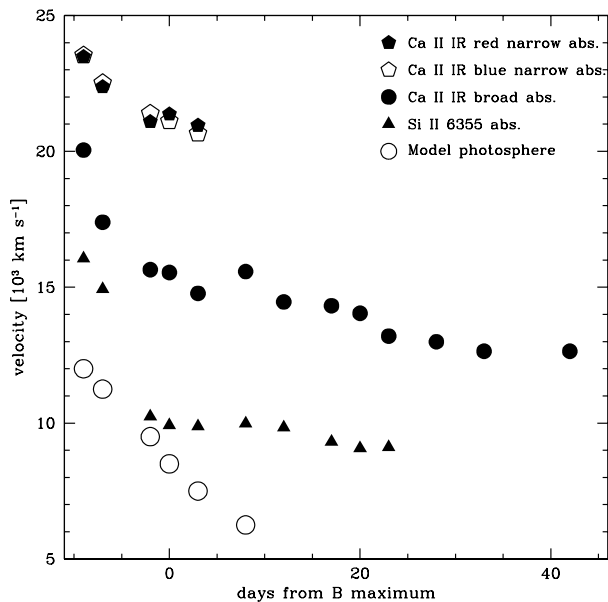


Figure 2. Time evolution of the observed velocity of the Ca II IR triplet components, the Si II 6355Å line, and the photospheric velocity adopted in model calculations.

then of the disappearing of the Ca II features and the return to normal of the Si II line suggests that these events may be correlated. The behaviour of the Si II line may also be due to the presence of high-velocity material, which makes the line appear at bluer wavelengths than usual at first. Later, as this material becomes optically thin, the line recovers its typical profile.

3 MODELLING THE SPECTRA AND IDENTIFYING THE DETACHED FEATURES

In order to locate accurately the regions responsible for the detached features and to describe realistically their physical properties, we modelled the sequence of spectra of SN 1999ee with our Montecarlo code (Mazzali & Lucy 1993; Lucy 1999; Mazzali 2000). As a first step, we tried to obtain reasonable matches to each spectrum across the observed wavelength range. We used a standard explosion model (W7, Nomoto et al. 1984), and adjusted its 1D abundances to achieve a good match to the observations. We then modified the density and abundance distributions to reproduce the narrow Ca II features and the behaviour of the Si II line.

We have modelled all 6 available spectra, starting from the first one, at day -9, and until day +8. This covers the time when the spectral anomalies are present. We tried to reproduce the global properties of the spectra, neglecting the narrow Ca II features or the fast Si II line when present. This step was necessary in order to define quantities such as the luminosity and the photospheric velocity, which we can compare to the observed velocities plotted in Fig.2.

The series of synthetic spectra is shown in Fig.3. The earliest spectra are sufficiently well reproduced, but then the

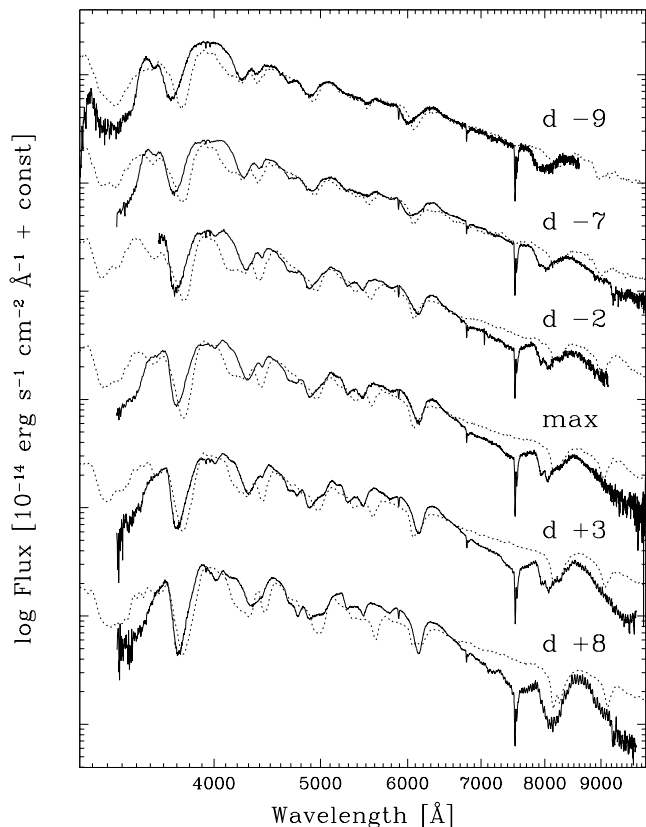


Figure 3. Synthetic spectral sequence (dotted lines) using W7 densities and abundances.

synthetic spectra become rapidly worse. Even at the earliest epochs, close inspection reveals defects caused by neglecting of the high-velocity components. In particular, looking at the first spectrum, the Ca II IR triplet and H&K doublet, and the Si II 6355Å line are significantly too red in the model, while other features such as the absorptions near 4250 and 4900Å, which are dominated by Fe III lines at this epoch, are correctly reproduced. This behaviour repeats at other epochs, including those where the narrow components are present.

4 AN ABUNDANCE ENHANCEMENT?

Based on the models above, we tried to reproduce the various spectral anomalies by modifying the distribution in velocity space of the elements involved. Guided by the observed spectra, we introduced regions of increased abundances (relative to W7) of Si, Ca, and Fe at well defined velocities, trying to improve the synthetic spectra.

The reason we experimented with the Fe abundance, as well as those of Si and Ca, is that Hatano et al. (1999) attribute a feature near 4700Å seen in SN 1994D to high-velocity Fe II (multiplet 48) absorption. A similar feature is observed in SN 1999ee, although the simple W7-based models seem to reproduce that region reasonably well, at least compared to the Fe-dominated region near 4300Å.

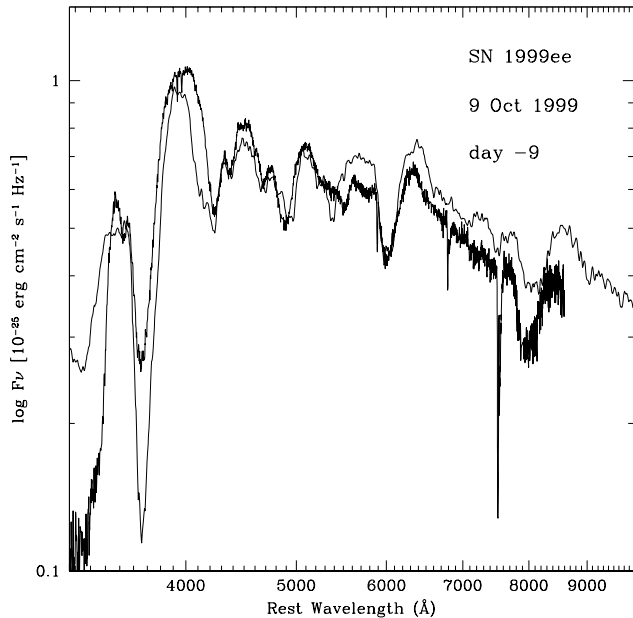


Figure 4. Model for the Oct. 9 spectrum with increased abundances of Si, Ca, and increased optical depth of Fe II lines (thin line).

Starting from the first spectrum, we increased the abundance of Si by factors between 5 and 20 at velocities between about 16000 and 22000 km s⁻¹, and that of Ca by a factor of about 20 at velocities larger than about 20000 km s⁻¹. It is however not possible to reproduce the narrow features near 4700Å by simply increasing the Fe abundance. This in fact generates both Fe III and Fe II lines at high velocity, but there are Fe III-dominated absorptions, like that at 4250Å, that do not show high-velocity components. Therefore, we increased only the opacity of the Fe II in order to get a qualitative assessment of the possible role of high-velocity Fe II. The opacity of Fe II was increased by factors of $\sim 10^4$ at $v > 28000$ km s⁻¹. The results for the earliest spectrum are shown in Fig.4. The position of the Si II and Ca II lines is now reproduced much better, and the absorption near 4700Å is now modelled as high-velocity Fe II, demonstrating the plausibility of the hypothesis that high-velocity components are responsible.

If high-velocity features are to be taken seriously it should be possible to reproduce their effect on the spectra consistently at all epochs. Therefore, we applied the enhancements to the abundances of Si, Ca, and the Fe II opacity in the velocity shells defined above, at all other epochs. The results are shown in Fig.5, while blow-ups of the Si II and Ca II IR regions are shown in Figures 6 and 7, respectively. Remarkably, the adopted high-velocity distribution seems to give an excellent description of all observed peculiarities. The Si II line is still blue on day -7 ($\lambda \sim 6000\text{Å}$), but in the next epoch, day -2, it has shifted by at least 150Å to the red. This is due to the reduced opacity of the high-velocity Si region, as the photosphere moves further inwards. The line is then reproduced well at all later epochs. As for Ca II, in the two earliest epochs the introduction of the high-abundance region leads only to a blueward shift of

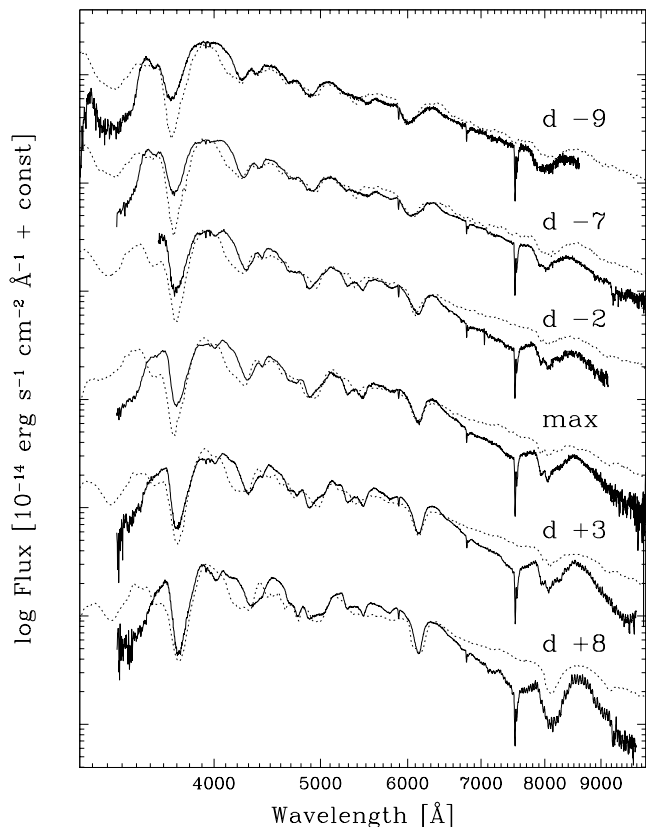


Figure 5. Synthetic spectral series using the abundance distribution discussed in Sect.4 (dotted lines).

the absorption, since $v(ph) \sim v(det)$. At later epochs, however, the Ca II high-abundance region becomes detached. Since the velocity separation of the high-abundance region from the photosphere is much greater than the velocity separation of the two strongest lines in the triplet, which is in turn larger than the velocity width of the high-velocity region, the two narrow absorptions are formed. They persist - at the correct wavelength - until the last epoch, when they disappear as their optical depth becomes too small. As we remarked earlier, Ca II H&K does not show distinctly detached features. However, the introduction of the high-velocity component leads to significant line optical depth at high velocity, causing the line to shift bluewards. This is the case for all the six spectra modelled. Finally, the feature we tentatively attributed to Fe II is also reproduced very accurately in all except possibly the last epoch.

The modified abundances imply that the regions involved are dominated by Si ($\sim 90\%$ by mass), and have a high abundance of Ca ($\sim 10\%$ by mass). The Fe abundance can be low ($\sim 1\%$ by mass), but the ionisation degree of Fe must favour Fe II over Fe III. Wang et al. (2003) obtained rather similar values for SN 2001el. These abundances would imply significant burning of the outer layers of progenitor white dwarf (WD).

Burned material such as Si may be produced at very high (but not the highest) velocities if the explosion mechanism was a delayed detonation (e.g. Höflich & Khokhlov

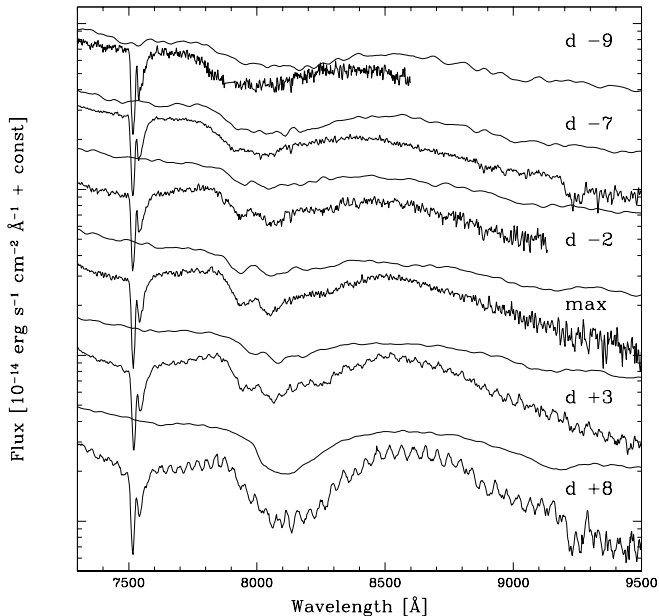


Figure 6. A blow-up of the Ca II IR triplet region from the series of spectra shown in Fig.6. The models are shown here as thin continuous lines to highlight the line profiles.

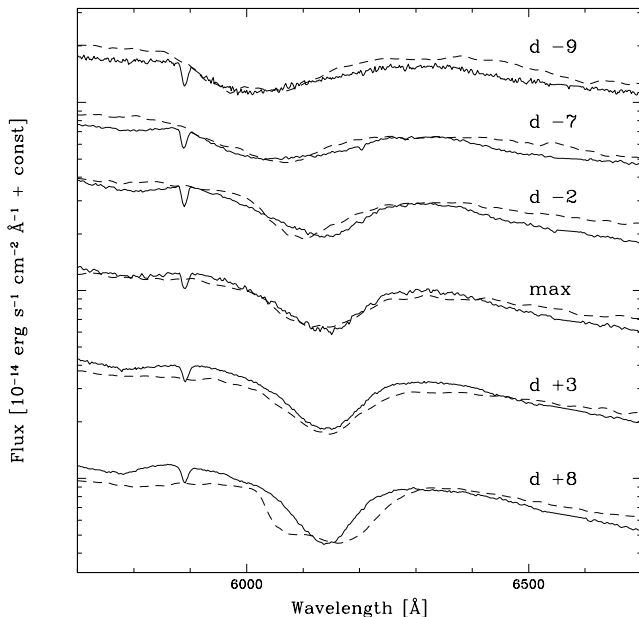


Figure 7. A blow-up of the Si II line region from the series of spectra shown in Fig.6.

1996; Iwamoto et al. 1999). Alternatively, in the deflagration model, a thin He envelope ($0.01M_{\odot}$) could be located in the outermost part of the WD and be burned by a precursor shock during the explosion; for a layer with densities as low as $\sim 10^5$ and $\sim 10^6 \text{ g cm}^{-3}$, Si-rich and Ca-rich ele-

ments are synthesized, respectively (Hashimoto et al. 1983; Nomoto 1982b).

An alternative possibility might be that the outermost shells have a higher abundance of these species, reflecting the metallicity of the progenitor (Lentz et al. 2000). The required abundance ratios seem however to high for this scenario: even in the most metal-rich situation Lentz et al. (2000) consider, the abundance of Ca would be much less than the 10% by mass which is required in our models.

Another relatively unexplored possibility is that He shell flashes during the pre-SN evolution might produce elements such as Mg, Si, and Ca. The He flash is stronger for slower accretion, becoming stronger as the white dwarf approaches the Chandrasekhar mass (Nomoto 1982a).

5 A DENSITY ENHANCEMENT?

A different possibility to obtain high-velocity features is an overall increase in density above what is predicted by W7. This may also help explaining the low ionisation degree of Fe at high velocity. Therefore, in the next set of models, we increased the density in a few shells at high velocity, leaving the original W7 abundances unchanged.

In these models, there is much less freedom to change parameters to obtain a good fit, since the test is to determine whether changing the density in a number of shells can lead to all high-velocity features being reproduced consistently, and to verify that models with this density change reproduce the observed spectra at all epochs.

Since the high-velocity features appear at $v > 16000 \text{ km s}^{-1}$, we increased the density of the corresponding shells with respect to W7, without changing the abundances. We selected a set of density changes which allowed us to get a good match of the day -9 spectrum. In this model, shown in Fig. 8, the density was increased by a factor 1.5 at $16750 < v < 20750 \text{ km s}^{-1}$, by a factor 8 at $20750 < v < 22500 \text{ km s}^{-1}$, and by a factor 5 at $v > 22500 \text{ km s}^{-1}$. The extra mass contained in the ‘bump’ is $0.1M_{\odot}$. This is a large increase of the mass at the highest velocities. Model W7, in fact, has only $\sim 0.07M_{\odot}$ of material above 16750 km s^{-1} .

Increasing the density leads to much broader and bluer Ca II and Si II lines. The spectrum is very well reproduced, but the 4700\AA feature is not, although the ionisation of Fe is indeed reduced at the velocities where the density is enhanced. The Ca II IR triplet becomes broad, but it is still narrower than the observed profile.

We used this modified density distribution to compute spectra at all observed epochs. The results are shown in the sequence of Fig.9. The change in density is able to explain both the sudden redward shift of the Si II line and the appearance of the narrow components in the Ca II IR triplet. The fact that the timing of the change is correctly reproduced confirms that both the position and the amount of the modification are correctly estimated.

A weak high-velocity Fe II absorption appears at 4700\AA in the spectra near maximum light. An increase in the Fe abundance as well as in density seems to be necessary to reproduce the feature as Fe II, so we cannot confirm this identification.

The quality of the synthetic spectra when compared to

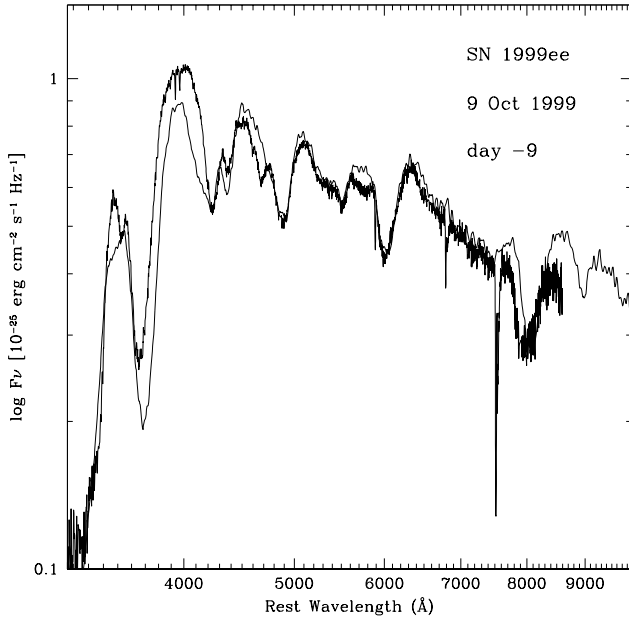


Figure 8. Model for the Oct. 9 spectrum with increased density at high velocity (thin line).

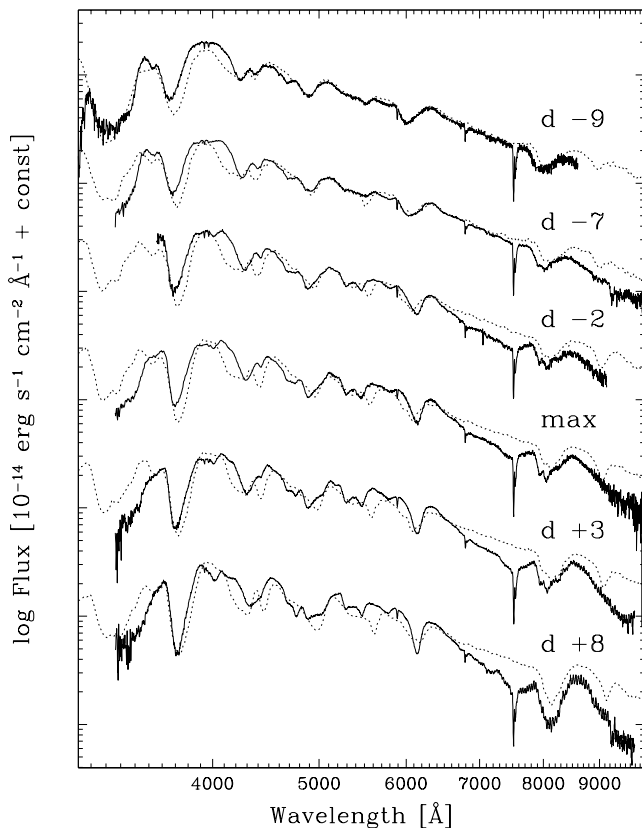


Figure 9. Synthetic spectral series using the increased density discussed in Sect.5 (dotted lines).

the observed ones suggests that an increase in density is a possibility that must be considered seriously. An overall variation of the density by this amount may occur if the explosion is not spherically symmetric, so that parts of the ejecta may be affected by burning differently from others. If these regions have sufficiently large angular scale, they may give rise to the observed spectral peculiarities. Polarisation measures in SN 2001el (Wang et al. 2003) may support this possibility.

6 INTERACTION WITH A CSM?

In the models in the previous section, the full width of the Ca II IR triplet in the earliest spectrum was not reproduced, even though the density was significantly enhanced. One possibility would be to add even more mass at the highest velocities. However, it is probably not reasonable to expect that the deviation from the spherically symmetric density structure can be much larger than what we have used. A different possibility to add mass at the highest velocities is the accumulation of circumstellar material.

If the SN ejecta interact with a circumstellar environment, it is most likely that the CSM composition is dominated by hydrogen. We tested different ways of adding hydrogen in the spectrum on day -9 , taking only thermal effects into account. In each test, the limiting value of the H mass was constrained by the strength of the synthetic H α line. H α is in fact not visible in the observed spectra.

First, starting from the modified W7 density distribution that we derived in the previous section, we introduced H uniformly in the ejecta at $v > 11250 \text{ km s}^{-1}$. This was done by simultaneously reducing the abundances of all other elements. With this method we obtained an upper limit for the H mass of $0.021 M_{\odot}$, corresponding to a H abundance of 4% H by mass, which is actually $\sim 50\%$ by number. Although H α is produced at this point, no changes are seen in either the Ca II or the Si II line profiles.

Then we assumed that only the outermost parts of the modified density structure contains hydrogen, 50% by mass, to simulate the piling up of CSM material, and increased this H shell inwards. It is sufficient to introduce H above 25000 km s^{-1} to see a change in the synthetic Ca II IR triplet. Although H α is not seen, the presence of H has an indirect influence on the spectra, making the Ca II IR triplet significantly broader. The overall spectrum is shown in Fig.10, and a blow-up of the Ca II IR region is shown in Fig. 11. The total H mass in this model is only $0.004 M_{\odot}$.

This can be explained as follows: since the electron density is significantly increased when even a relatively small amount of H is added, recombination is favoured. Since at the highest velocities Ca is mostly doubly ionised, once H is introduced the fraction of Ca II increases (by factors between 3 and 6 in the zones affected for the particular model we used). This leads to an increased strength of the Ca II lines and to the observed broader absorption. A second-order effect is also at play. A higher electron density means that photons have a higher probability of scattering off electrons. This results in a longer residence time of photons in the H-rich shells, and thus in turn in a higher probability that photons can interact with spectral lines. The effect of this is an increased line absorption - in all lines - at the highest

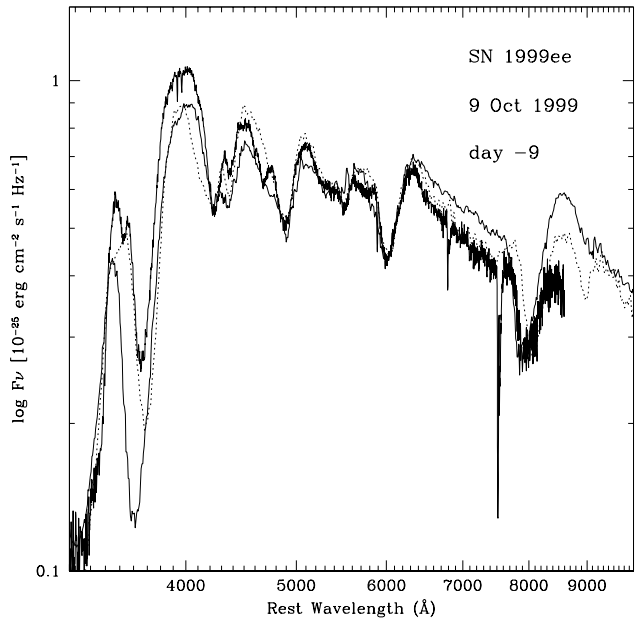


Figure 10. Model for the Oct. 9 spectrum using the increased density of Sect.5 but with an outer $0.004M_{\odot}$ of Hydrogen (thin line). The model without H shown in Fig.8 is also shown here as a dotted line for comparison.

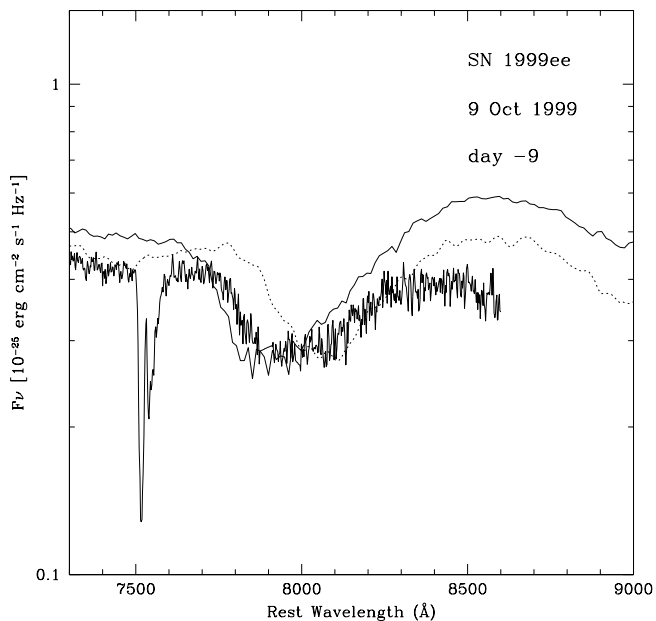


Figure 11. A blow-up of the Ca II IR triplet region from Fig.10.

velocities, since that is where the electron density effect is at play. Since the Ca II lines are the strongest in the optical spectrum, they are also the most affected. Electron scattering opacity is also responsible for the partial suppression of the peak near 4000 Å.

At later epochs, the photosphere becomes further re-

moved from the region where the hydrogen was added, and the spectra are therefore not affected: the results are similar to those of Figure 9.

A necessary condition for hydrogen to affect the Ca II IR triplet is that the CSM and the SN ejecta are well mixed, at least in a narrow region between 25000 and 28000 km s^{-1} . The abundance of Ca in the CSM (taking solar as a typical value) is in fact too small to give rise to the line opacity which is required to reproduce the observed line broadening, so the line must be due to Ca from the SN ejecta. Thorough mixing may not be easy to achieve, but what is required here affects only a very small mass ($\sim 0.006M_{\odot}$), which may represent the interface between SN ejecta and CSM. In our model, this region contains $\sim 5\%$ Ca by mass.

These calculations cannot by themselves prove that the spectral peculiarities of SN 1999ee are – at least partially – due to an outer shell of H, especially since the H mass we used is smaller than the mass added by modifying the density profile (Gerardy et al. (2004) use $0.02M_{\odot}$ of H-rich material to broaden the Ca II IR triplet in SN 2003du, but those spectra do not show a broad Si II line, and in any case the effect they predict on that line is the opposite, namely a narrowing of the line). However, our results suggest that the presence of H-rich material can have far-reaching effects on the spectra, even if the Balmer lines are not themselves visible. An accurate study of the effect of H at high velocity will be the topic of future work.

7 DISCUSSION

We have shown that a modification of the abundances or an increase of the mass at the highest ejecta velocities can explain the high velocity features observed in the spectrum of SN 1999ee. The former situation might result from the nuclear burning reaching the outermost layers of the white dwarf. The outer layers must contain mostly products of incomplete burning, in particular Si, and some Fe. A change of the density structure could be due to either a deviation, possibly not spherical, from the average properties of the explosion, or to the accumulation of CSM material, or perhaps to both factors.

If the bump in density is due to SN material, it should contain $\sim 0.1 M_{\odot}$ of material. This is a rather large change. However, it is quite possible that what we can reproduce as a ‘density bump’ in one-dimensional models may actually be just a ‘density blob’ in three dimensions. Attempts have been made to model detached components as blobs in 3D (Kasen 2004). Unfortunately, spectropolarimetric data are not available for SN 1999ee, and so the geometry cannot be constrained, resulting in a degeneracy of solutions.

Qualitatively, in order to reproduce the observed spectral signatures, any blob must not be too small in size compared to the size of the photosphere. If one such blob is observed because it happens to lie along our line-of-sight, chances are that at least a few others are ejected as well. To support this, we note that two separate sets of high-velocity features were observed in SN 2000cx. It is a matter of probability to determine the optimal number and size of such blobs so that they are only observed in a few SNe. Unfortunately, the blobs become too thin to be visible as narrow emissions in the nebular spectra, where a head count would

be much easier since radiative transport is not an issue. The question whether a global density enhancement or a blob are to be preferred could be resolved with more spectropolarimetric observations. Both SN 2001el (Wang et al. 2003) and SN 2004dt show polarisation at early epochs, which may support the blob hypothesis, as might the fact that most well-observed SNe Ia near maximum do not show high-velocity features. These seem to be a much more common property of SNe Ia at earlier epochs (~ 1 week before maximum or earlier, Mazzali et al. , 2005, in preparation). Perhaps, while broad early absorptions reaching high velocities may be the result of ejecta-CSM interaction, narrow high-velocity absorptions near maximum could be the signature of blobs.

If we assume that H-dominated CSM material is piled up at the highest velocities, the enhanced electron density causes the ionisation degree to be lower in those regions. Line broadening is then caused by the increased optical depth of the Ca II IR triplet.

In view of the mounting evidence that SNe Ia can indeed interact with CSM (e.g. Hamuy et al. (2003); Deng et al. (2004); Kotak (2004)). It will be interesting to verify whether models where the only density enhancement is due to H-rich material can also reproduce the high-velocity features.

ACKNOWLEDGMENTS

This work was partly supported by the European Research and Training Network 2002-2006 "The Physics of Type Ia Supernovae" (contract HPRN-CT-2002-00303), and by the grant-in-Aid for Scientific Research (15204010, 16042201, 16540229) and the 21st Century COE Program (Quests) of the MEXT, Japan. We thank the anonymous referee for useful remarks that helped improving the presentation of the paper.

REFERENCES

- Branch, D., et al, 2004, ApJ, 606, 413
 Deng, J., et al, 2004, ApJ, 605, L37
 Gerardy, C.L., et al, 2004, ApJ, 607, 391
 Hamuy, M., et al., 2002, AJ, 124, 417
 Hamuy, M., et al., 2003, Nat, 424, 651
 Hashimoto, M.-A., Hanawa, T., and Sugimoto, D., 1983, PASJ, 35, 1
 Hatano, K., Branch, D., Fisher, A., Baron, E., and Filippenko, A.V., 1999, ApJ, 525, 881
 Höflich, P., and Khokhlov, A., 1996, ApJ, 457, 500
 Iwamoto, K., Brachwitz, F., Nomoto, K., Kishimoto, N., Umeda, H., Hix, W.R., and Thielemann, F.-K., 1999, ApJS, 125, 439
 Kasen, D., Nugent, P., Thomas, R.C., and Wang, L., 2004, ApJ, 610, 876
 Kotak, R., Meikle, W.P.S., Adamson, A., and Leggett, S.K., 2004, A&A, 413, 301
 Lentz, E. J., Baron, E., Branch, D., Hauschildt, P. H., and Nugent, P. E., 2000, ApJ, 530, 966
 Li, W. et al, 2001, PASP, 113, 1178
 Lucy, L.B., 1999, A&A, 345, 211
 Mazzali, P.A., 2000, A&A, 363, 705
 Mazzali, P.A., & Lucy, L.B. 1993, A&A, 279, 447
 Nomoto, K., 1982a, ApJ, 253, 798
 Nomoto, K., 1982b, ApJ, 257, 780
 Nomoto, K., Thielemann, F.-K., & Yokoi, K., 1984, ApJ, 286, 644
 Phillips, M.M., 1993, ApJ, 413, L105
 Stritzinger, M., et al., 2002, AJ, 124, 2100
 Thomas, R.C., Branch, D., Baron, E., Nomoto, K., Li, W., and Filippenko, A.V., 2004, ApJ, 601, 1019
 Wang, L. et al, 2003, ApJ, 591, 1110

This paper has been typeset from a \TeX / \LaTeX file prepared by the author.